IEEE Access
Multidisciplinary Rapid Review Open Access Journal

Received 11 March 2025, accepted 5 April 2025, date of publication 10 April 2025, date of current version 22 April 2025.

Digital Object Identifier 10.1109/ACCESS.2025.3559619

RESEARCH ARTICLE

Real-Time EEG Signal Analysis for Microsleep Detection: Hyper-Opt-ANN as a Key Solution

MD MAHMUDUL HASAN [1], MD NAHIDUL ISLAM [1], NORIZAM SULAIMAN [1], MIRZA MAHFUJ HOSSAIN [2], AND JORGE M. MENDES [3]

[1]Faculty of Electrical and Electronics Engineering Technology, Universiti Malaysia Pahang Al-Sultan Abdullah, Pekan 26600, Pahang, Malaysia
[2]Department of Computer Science and Engineering, Jashore University of Science and Technology, Jashore 7408, Bangladesh
[3]Comprehensive Health Research Centre (CHRC), NOVA Medical School, Universidade NOVA de Lisboa, 1169-056 Lisbon, Portugal

Corresponding author: Jorge M. Mendes (jorge.mendes@nms.unl.pt)

This work was supported in part by the Faculty of Electrical and Electronics Engineering Technology, Universiti Malaysia Pahang Al-Sultan Abdullah, under Grant PDU233212. The present publication was funded by Fundação Ciência e Tecnologia, Instituto Público (IP) national support through UID/04923 - Comprehensive Health Research Centre.

This work involved human subjects or animals in its research. Approval of all ethical and experimental procedures and protocols was granted by the IIUM Research Ethics Committee (IREC) under Application No. IIUM/504/14/11/2/ IREC 2023-239.

ABSTRACT Microsleeps are brief lapses in awareness that pose significant risks, particularly in activities requiring continuous attention, such as driving. These episodes are common in sleep-deprived individuals and can lead to catastrophic outcomes. Electroencephalography (EEG) is a promising technique for detecting microsleeps due to its high temporal resolution, allowing real-time brain activity monitoring. The study aims to develop a lightweight version of the model to reduce computational costs and provide faster detection, enabling quicker intervention to prevent accidents in safety-critical environments. We propose a customized deep learning model, Hyper-Opt-ANN, designed to detect microsleep episodes from EEG signals. The model is evaluated across five time windows (1 second, 2 seconds, 3 seconds, 4 seconds, and 5 seconds), with the 4 seconds window showing the best performance. The Hyper-Opt-ANN model achieved a significant accuracy of 97.33%, demonstrating its efficacy and potential for accurate microsleep detection using EEG signals. This method significantly outperforms traditional approaches and has potential applications in safety-critical domains. This study demonstrates the feasibility of using EEG signals and advanced deep learning models for detecting microsleep and enhancing safety in high-risk environments.

INDEX TERMS Microsleep detection, EEG signal, hyper-Opt-ANN, parameter optimization, time-window selection.

I. INTRODUCTION

Microsleeps are brief unconscious lapses in awareness during which an individual momentarily falls asleep and experiences a temporary pause in performance [1]. While they are more common when a person is sleep-deprived, also can occur when person experiences sleep deprivation or engages in monotonous activity [2] and typically happen without warning [3]. However, a recent accident due to fatal microsleep has triggered cascading consequences, including an incident that resulted in over 200 deaths and more than 400 injuries [4]. According to estimates from the NSC (National Safety Council), drowsiness causes more than 1,00,000 road accidents worldwide each year, resulting in over 800 deaths and 71,000 injuries [5].

The number of sleep-related traffic accidents can be considerably decreased by creating reliable techniques for assessing drivers' sleep-related performance deficiencies. A microsleep cycle is one important indicator of the start of sleep. It may be identified by its irregular and varied theta-wave pattern, which includes (a) a slowing of the frequency spectrum and (b) eyelids closed for up to 80% of the time. Whenever there are sudden changes from awake to sleep, these problems are typically seen [6], [7]. More precisely,

The associate editor coordinating the review of this manuscript and approving it for publication was Ghulam Muhammad.

this is characterized by drooping eyes, head swaying, and sluggish, sporadic eyelid closures and happens when there are abrupt changes between waking and sleep.

In recent years, researchers have identified various methods to assess driving conditions in recent years. Among these, commonly explored physiological signals include EEG [8], electrooculography (EOG) [9], and electrocardiography (ECG) [10]. These techniques enable proactive intervention and early detection. The human brain's functional layout has been widely studied using functional magnetic resonance imaging (fMRI), which has important therapeutic applications. However, fMRI could be too costly and impractical for detecting driving fatigue in real-world driving scenarios [11]. Although functional near-infrared spectroscopy (fNIRS) is used in confirmatory studies, it cannot capture signals from certain brain regions and has a lower temporal resolution than EEG or event-related potentials. Additionally, a relatively recent categorization approach for fNIRS has been extensively utilized to monitor the incidence of neuroplasticity after neurorehabilitation and neurostimulation; it is inexpensive, portable, and safe, and produces low noise compared to fMRI [12], [13]. But the fNIRS is mostly confirmatory research due to its low temporal resolution compared to EEG or event-related potential and the inability to get signals from the brain area. Since EEG directly detects brain activity with a high temporal resolution, it is a popular and intriguing modality because of its exceptional temporal resolution of changes in brain activity. EEG has the finest temporal resolution among all the methods used in brain research. When full-head dense electrode arrays are used, it offers high spatial resolution. Yet as spatial resolution increases, expenses rise, and usability and convenience are diminished [14]. Compared to other methods like fNIRS, EEG offers superior temporal resolution, making it more effective in detecting rapid changes in brain activity associated with microsleep.

Numerous studies have utilized machine learning (ML) to detect the high temporal resolution in EEG data. The primary goal of these studies was to assess various techniques for feature extraction, selection, and reduction to develop models for detecting microsleeps [15]. However, the challenge lies in effectively preserving the complex relationships between EEG signal characteristics and machine learning algorithms, which are crucial for accurately detecting microsleeps. Additionally, the invariance of selectivity makes it difficult for machine learning models to capture the dynamics of micro-voltages, as the features are manually selected by algorithm or system designers. Feature selection plays a crucial role in determining the performance of a model [16]. Feature allows models to extract relevant information dynamically, leading to a more nuanced understanding of data patterns. Additionally, deep learning (DL) algorithms provide a comprehensive solution due to its ability to capture more complex information by autonomously analyzing, and capturing information. Greater focus could be placed on developing models using DL to enhance microsleep detection performance [16], [17]. However, DL models often suffer from high computational costs, extended detection times, and increased model complexity, which can limit their practical application in real-time microsleep detection systems.

Therefore, the utilization of proposed Hyperparameter optimized ANN (Hyper-Opt-ANN) model enhances model performance by fine-tuning key parameters, thus reducing computational complexity, while maintaining high accuracy and minimizing detection latency, which are critical for real-time microsleep detection in EEG data analysis. The Hyper-Opt-ANN model provides an optimal trade-off between accuracy and computational efficiency, making it more suitable for classifying low-dimensional EEG features than CNNs and RNNs.

The following is a summary of the findings from the study conducted in the investigation:

- i We introduce an optimized architecture, Hyper-Opt-ANN, that effectively identifies the microsleep states utilizing EEG signals. In the proposed method, we modified several high-level parameters, reduced the number of parameters, and simplified the architecture. These changes improved the model performance on EEG signals and shortened the computational duration of the training process.
- ii The experiment is conducted using Fast Fourier Transform (FFT) features. Utilizing FFT features can reduce computational complexity while preserving essential frequency information. This approach enhances the accuracy of the analysis by capturing key spectral components without the need for extensive time-domain processing.
- iii The experiment has used five different time windows (1s, 2s, 3s, 4s, and 5s), demonstrating the resilience and practicality of the proposed approach, and determining the best time window to identify microsleep utilizing the proposed approach.
- iv The performance of the proposed model is thoroughly assessed quantitatively to provide a clear understanding of its relevance and demonstrate that it performs better than existing techniques for microsleep detection.

The remainder of this paper is structured as follows. Section II presents the relevant literature on earlier comparable studies. Section III provides a full description of the experimental data, including methodology, data collection, and preparation. Section IV provides a detailed overview of the study process, including characteristics, the suggested model description, and model assessment metrics. Section V presents the results, while Section VI provides a discussion, including a comparison with related studies and also outlines the limitation of this study. Finally, Section VII concludes the paper.

II. LITERATURE REVIEW

Multiple techniques are used in this field of study to diagnose car drivers' microsleep early. To detect multimodal aspects, Du et al. [18] extracted facial emotions from the driver's pulse rate using a wrist monitor equipped with an RGB camera. Li et al. [19] described a technique that combined EEG and EOG measurements. Their suggested solution reduces error rates to 5% while increasing the accurate classification rate of fatigue levels to 80.6% for alert, sleepy, and severely drowsy circumstances. Ramzan et al. [20] suggested an attribute fusion and transfer learning strategy based on EEG and cervical EMG data to identify driver weariness. Their investigation demonstrates a greater rate of detection than the standard support vector machine (SVM) model. In another study, manual identification of microsleep episodes by tracking three video streams of driving scenes and subjects' eye movements was correlated with electrocardiogram (ECG) data, revealing that heart rate decreased and heart rate variability increased during these episodes [21].

Wali et al. [22] presented a system for detection that correlated alertness, fatigued, and occupied states using EEG signal. This study presented and amplitude spectrum of the three bands (theta, alpha, and beta) of the EEG signal which has been proposed along with the hybrid scheme based on DWT and FFT. Fusions of the above two methods give more significant results on extraction of centroid and PSD features under ANOVA analysis, and maximum accuracy of 79.21% using sym8 and subtractive fuzzy inference system for PSD feature with an average sensitivity of 82.09% and of 70.36%. However, a multi-mode EEG analysis-based automatic tiredness detection system was introduced in [23]. This study utilized multiple features and ANN classification model and achieved an accuracy of 83.6% to detect drowsy conditions. Another study in [24] employed optical stimulation and steady-state visual elicited possible signals on drivers with different scan times. The Fourier transform approach was applied to feature extraction. Three discriminant analysis classifiers were then used to classify the retrieved feature. The study in [25], utilized an LSTM based hybrid model for EEG-based drowsiness detection integrates tunable Q-factor wavelet transform (TQWT) and deep learning-based features, achieving an average accuracy of 94.31%. Jacobé De Naurois et al. [26] effectively utilized ANN model for detecting and predicting driver drowsiness by analyzing physiological, behavioral, and performance indicators. However, Laurent et al. [27] underscore the critical role of time-window duration in enhancing the speed and accuracy of detecting fatigue studies.

Current methods that do not rely on EEG for monitoring microsleep typically use facial recognition technologies. These methods involve detecting key points on the face and extracting various features from them to assess signs of microsleep. The process analyzes subtle facial movements or expressions indicative of the onset of microsleep, providing an alternative approach to traditional EEG-based monitoring [28], [29]. Additionally, algorithms are employed to track and monitor eye movements, helping to detect signs of microsleep through subtle changes in eye behaviour [30], [31]. Despite their potential, these approaches may lack consistency, with their effectiveness being heavily influenced by factors like dim lighting or foggy environments.

Based on the review of existing studies, it is evident that various techniques and models have been employed to detect microsleep using EEG, multimodal signals and other techniques. Additionally, recognizing that no specific time window has been universally established for effective microsleep detection, this study conducted a comprehensive investigation to identify the optimal time window for analysis. This ensured the most accurate and reliable detection results. Furthermore, this study implemented the lightweight Hyper-Opt-ANN model for faster and more effective microsleep detection, ensuring real-time applicability by reducing computational complexity while maintaining high accuracy.

III. EXPERIMENTAL DATA DESCRIPTION

A. PARTICIPANTS AND EXPERIMENTAL PROTOCOL

Fifteen participants were chosen to participate in the EEG signal collection events, including professors, postgraduate students, and undergraduate students. They ranged in age from 21 to 58 years and had no prior medical history. All participants were chosen solely from the Pekan Campus of the Universiti Malaysia Pahang Al-Sultan Abdullah. Before the trial began, they were told not to take any medication or use any drugs, including alcohol or coffee. The subjects had normal or correct eyesight and no medical history of neurological, physical, or mental illness. All participants provided informed consent before the commencement of the experiment, allowing the use of their data for this study. The IIUM Research Ethics Committee granted ethical permission to conduct this study (IREC 2023-239). The research study was conducted at the Faculty of Electrical and Electronics Engineering Technology, Universiti Malaysia Pahang Al-Sultan Abdullah, in the Signal Processing Laboratory and Applied Electronics and Computer Engineering Laboratory. For the participants in the trial, these laboratories offered a distraction-free setting where they could focus throughout the sessions. To ensure participants' relaxation, the experimental conditions were meticulously managed to preserve a calm environment, free from any noise disruptions and a moderate ambient temperature. To reduce the possibility of noise or undesirable signals throughout the experiment, the subject was told to assume a comfortable position and remain still, neither moving nor blinking their eyes [32].

B. DATA ACQUISITION

Unicorn Hybrid Black, an eight-channel wearable EEG headset device, was used to collect the EEG data, as shown in Fig. 1. Comprehensive details regarding the functionality and specifications of this device are extensively discussed in reference [27]. The apparatus was sampled at a rate

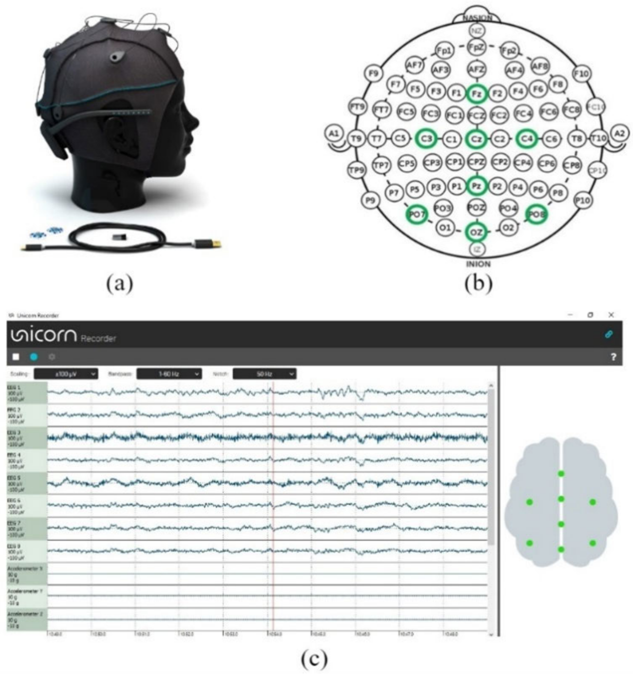

FIGURE 1. **Unicorn Hybrid Black headset device used to collect the EEG data used in this study. (a) Eight-channels wearable EEG headset. (b) Position of the eight electrodes Unicorn Hybrid Black (marked in green) used in this study, based on the international 10–20 system. (c) User interface of Unicorn Suite software while recording participants' data.**

of 250 Hz per channel, with a resolution of 24 bits. Version 1.18.0.2085 of the licensed UnicornSuite software was used to evaluate and collect data. As shown in Fig. 1(a), an eight-channel wearable EEG headset device, The Unicorn Hybrid Black gadget, was connected to a PC via the built-in Bluetooth connection. Eight EEG signals were captured from specified electrode locations: Fz, C3, Cz, C4, Pz, PO7, Oz, and PO8. Fig. 1(b) shows the positions of the channels, while Fig. 1(c) depicts the user interface incorporated into the Unicorn Suite program. Fig. 2 depicts the laboratory data-collection setup, and Fig. 3 illustrates the occurrence of an individual microsleep episode.

C. DATA PREPARATION

Many studies have utilized EEG bands associated with microsleep; however, band-wise analysis may overlook cross-frequency interactions. Therefore, the Karolinska Sleepiness Scale (KSS) [33] was employed in this study to provide a subjective measure, allowing for a more comprehensive assessment of microsleep beyond EEG band-wise analysis. Incorporating KSS enables the validation of EEG-derived microsleep detection with self-reported awake and slumber levels, enhancing the reliability of the findings. All fifteen participants, each undergoing a session lasting twenty to twenty-five minutes, were asked to fill out the KSS to assess their level of slumber.

The numbers 0 (Wakefulness) and 1 (Microsleep) represent the two classes that constitute the validation set. Accordingly, this study requires distinguishing them as either wakefulness or microsleep. A value of less than seven is associated with a KSS value of "‘0", whereas a value greater than or equal to seven is associated with a KSS value of "‘1". At least one investigator closely monitored the participants throughout the study to ensure data quality and reliability. This monitoring process included verifying the participants' physical and behavioural conditions and cross-checking them against their self-reported KSS values. This diligent oversight helped eliminate discrepancies and maintain consistency in the classification of wakefulness and microsleep. Although every participant was responsible for care- fully inputting their KSS value, the investigators recognized that there may be occasional discrepancies. Despite this, the investigators implemented rigorous monitoring and cross-checking procedures to minimize errors and ensure the reliability of the KSS data provided by the respondents. For a certain degree of drowsiness, one participant may input a KSS number greater than or equal to seven, whereas another participant may provide a KSS value of less than six.

IV. METHODOLOGY

The objective of this research is to develop a high-performance, intelligent, early stage microsleep detection technique for drivers. A crucial element is the extraction of characteristics from the EEG signals [34]. EEG signals typically contain complex data; therefore, FFT is applied in this investigation to extract frequency-domain features while preserving essential information. However, Fig. 4 illustrates the general steps of the proposed microsleep detection technique. A few phases comprise the suggested framework: gathering data, preprocessing, feature extraction and developing a new model with optimization parameters. Finally, to further validate the robustness of the developed model, a 5-fold cross validation is applied.

A. DATA PREPROCESSING

The data preprocessing procedure in this study comprises five critical stages to ensure the integrity and reliability of EEG signals for microsleep detection. The initial step involved the Exclusion of Low-Focus Periods, where 15 seconds were removed from both the beginning and end of each segment. This exclusion aimed to mitigate potential signal contamination caused by transitions in cognitive states and external disturbances, ensuring the extraction of high-quality data for analysis, this exclusion process is illustrated in Fig. 5.

Following this, Artifact Removal was performed using Independent Component Analysis (ICA) to eliminate unwanted signal components while preserving meaningful brain activity. ICA decomposed the EEG signals into independent components, each representing distinct neural and non-neural sources. Spatial and temporal criteria were applied to identify and discard artifactual components, particularly those arising from muscle activity, ocular movements, or environmental interferences. This step was

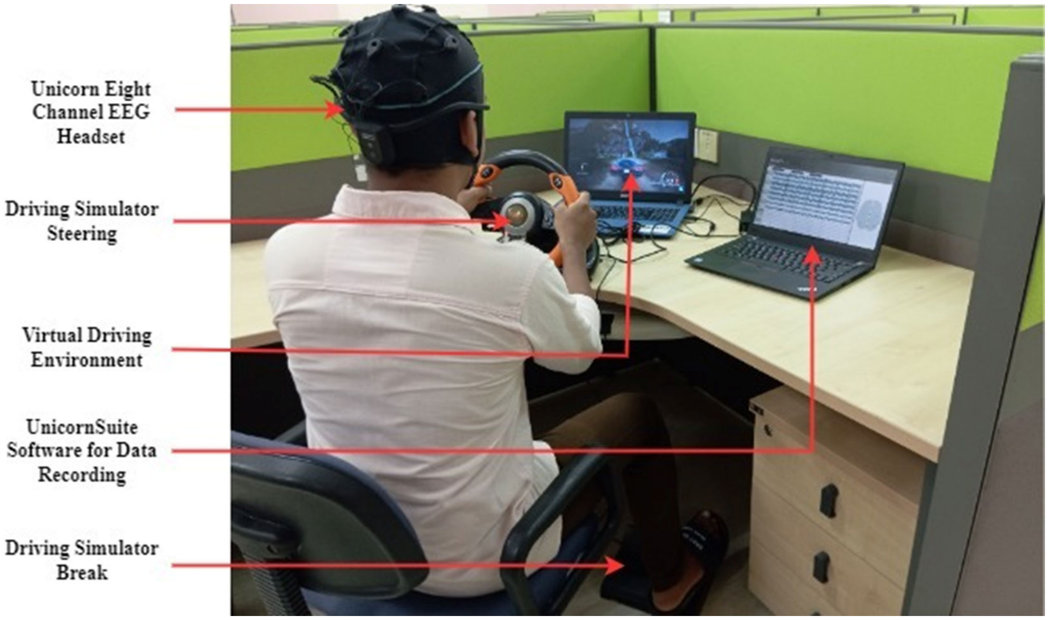

FIGURE 2. Laboratory data collection setup.

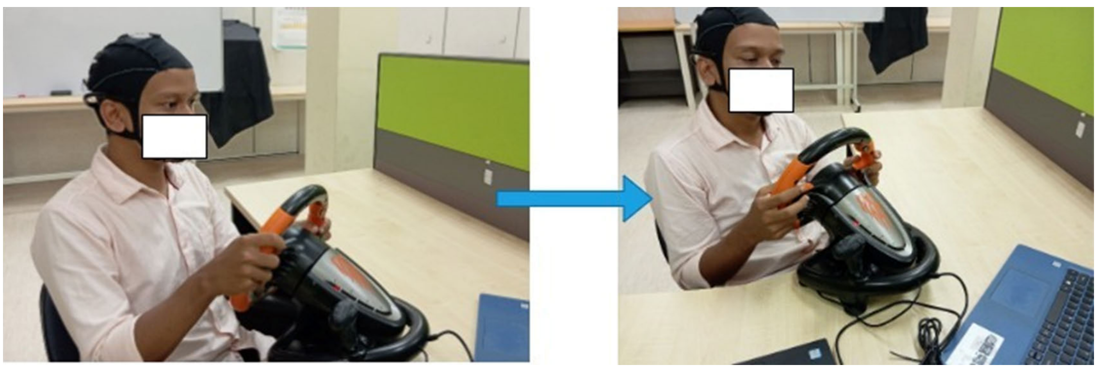

FIGURE 3. Example of microsleep occurrences captured during data recording on wheel.

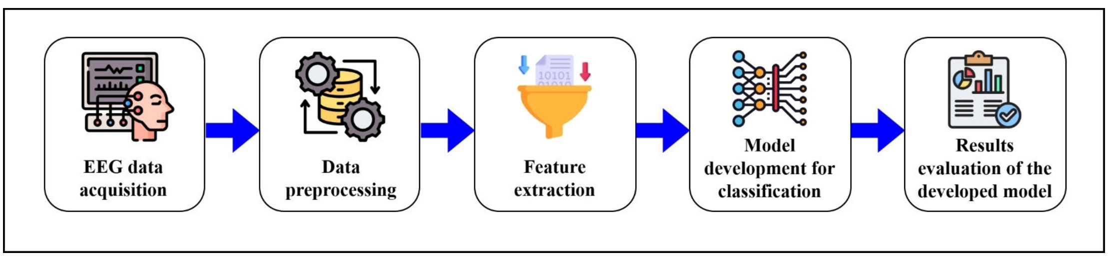

FIGURE 4. Overall design of the current study. The framework comprises five subsequent phases from acquisition of data to final assessment of proposed modelling strategy.

essential in minimizing distortions and improving the accuracy of downstream feature extraction.

The next stage focused on Noise Reduction, where a bandpass filter (0.5–45 Hz) was applied to remove undesired frequency components. This filtering process effectively suppressed low-frequency drifts and high-frequency noise, retaining only the relevant EEG frequency bands associated with microsleep detection. Improving the signal quality enhanced the model's robustness against noise-induced inconsistencies.

However, Fig. 6 illustrates the EEG signal processing pipeline, showcasing the effects of a bandpass filter and ICA

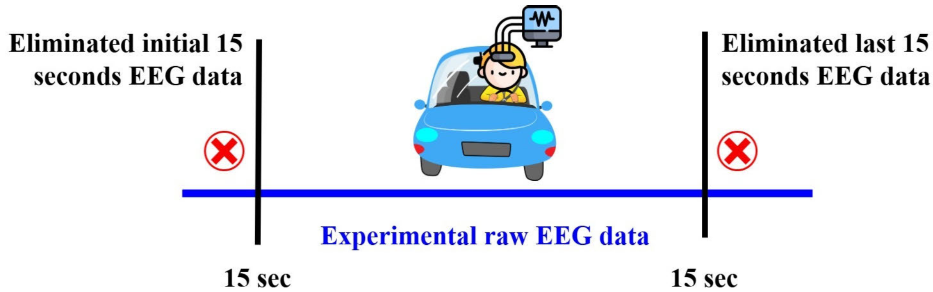

FIGURE 5. Mitigation of potential signal contamination caused by transitions in cognitive states and external disturbances. The first and last 15 seconds EEG signal were excluded from the analysis to ensure the extraction of high-quality data.

on eight EEG channels. The raw EEG signals are first filtered using a Bandpass filter to remove unwanted frequency components. Subsequently, ICA is applied to eliminate artefacts. The processed signals demonstrate reduced noise and enhanced signal quality, ensuring cleaner data for subsequent analysis.

Z-score normalization was employed to standardize the EEG data, addressing inter-subject variability and session-induced fluctuations [35]. Given the inherent differences in EEG amplitudes due to individual physiological factors, electrode placement, and recording conditions, z-score normalization ensured all features were centred around zero and scaled to unit variance. This transformation enhanced the comparability of EEG features across subjects and sessions, stabilizing the model's training process. As a result, the model demonstrated improved generalization capabilities in detecting microsleep states. The mathematical formulation of z-score normalization is presented in Eq. (1):

$$z = \frac{x - \mu}{\sigma}, \tag{1}$$

where z is the transformed value after standardization, x is the original value, μ is the average value across all samples, and σ is the measure of dispersion, representing how much the values deviate from the mean.

By implementing these steps, this study ensures a high-quality EEG dataset, reducing noise and artifacts while preserving essential neural information. These enhancements play a crucial role in optimizing the performance of classification models for accurate and reliable microsleep detection.

Lastly, each of the brief time windows, 1s, 2s, 3s, 4s, and 5s, created from the complete dataset was considered as each window as an observation. The simple rationale for choosing brief choice windows is to speed up the system and reduce the computing complexity, which will aid in identifying early microsleep conditions and reducing the number of car accidents caused by drivers. Fig. 7 shows the EEG data of five different time windows of a single participant in the time domain for both normal and microsleep conditions. As the time window increased, the signal patterns became more detailed for each sample, revealing additional fluctuations and variations in amplitude over longer durations. This progression allows for better visualization of the temporal dynamics and differences between the two conditions.

B. FEATURE EXTRACTION

This study uses the Fast Fourier Transform (FFT) to extract features from EEG signals by transforming them from the time domain to the frequency domain. In 1965, J. Fourier discovered the FFT, a Fourier transformation that is an enhanced version of the Discrete Fourier Transform (DFT). FFT enables rapid spectral decomposition of EEG signals, facilitates feature extraction, and identifies neural oscillations for EEG data analysis [36]. Fig. 8 presents the EEG signal and its corresponding frequency spectrum obtained by FFT. The FFT spectrum highlights the dominant frequency components, facilitating the identification of relevant oscillations. The mathematical formulation of the FFT is given by Eq. (2).

$$X_k = \sum_{n=0}^{N-1} x_n e^{\frac{-j2\pi kn}{N}}, \tag{2}$$

where X_k represents the FFT components, N represents the total number of EEG input samples, n denotes the total quantity of points in FFT and $k = 0, 1, 2, \ldots, N-1$.

C. FUNDAMENTAL CONCEPTS OF ARTIFICIAL NEURAL NETWORK (ANN)

In the 1980s, the neuroscience sector saw significant improvements in the usage of artificial neural networks (ANNs), a physiologically based intelligence model, which sparked a great deal of interest in comprehending the significance of neural network models [37]. Massive sets of algorithms that indicate artificial neural networks mimic the functions of neurons in the brain. Upon completion of learning and training, these networks can create relationships between extremely unusual nonlinear variables and provide complex, accurate, and reliable solutions to challenging problems [38]. The Feed-Forward Neural Network (FFNN), an array of connections of perceptron in which the output layer is not connected to a loop for connections to feedback or recurrent networks but rather in a forward unidirectional flow, is the most basic and straightforward of the two types

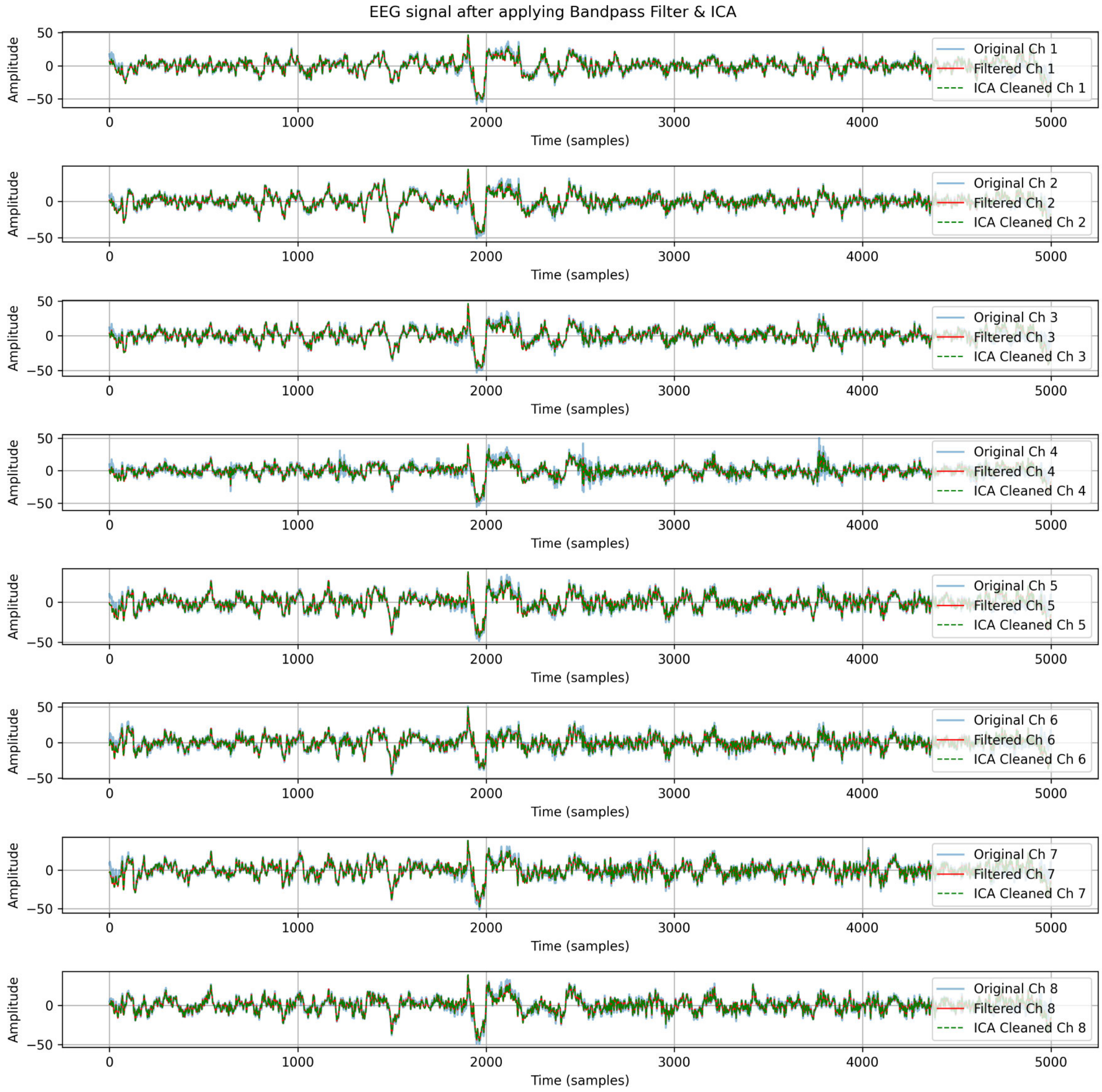

FIGURE 6. **EEG signal after applying Bandpass Filter and ICA. The raw EEG signals are first filtered using a Bandpass filter to remove unwanted frequency components and then Independent Component Analysis (ICA) is applied to eliminate artefacts. The processed signals are less noisy, enhancing signal quality for subsequent analysis.**

of neural networks [37]. Eq. (3) provides a mathematical representation of a basic neural network model:

$$h_\theta(x) = \frac{1}{1 + e^{-\theta x^T}}. \tag{3}$$

When the input is x, the parameter vectors are x and θ and the output is $h_\theta(x)$. The standard FFNN design is shown in Fig. 9(a). The feedback neural network, also known as the backpropagation ANN (BPANN), is another type of ANN frequently employed in supervised learning. Although it allows for the establishment of a loop where incorrect information is transmitted back for the repetitive alteration of weight values until the error can no longer be improved to obtain a more accurate output variable, this type of neural network shares an architectural structure with the FFNN. A typical archetypal structure of BPNN is shown in Fig. 9(b).

An ANN functions in a manner that is similar to the many interconnected neurones in the brain, wherein each node (point) is connected to every other node in the form of a route for cooperation. Each node in a neural structure may be assigned a weight using an ANN with a single hidden layer. The input data are sent to a neural network architecture as vectors during the training phase. When utilizing a BPANN, the output error is calculated and looped back into the network so that the weights can be changed iteratively using gradient descent to minimize the error based on expertise until it cannot be further improved. Once a bias value that yields an improved prediction is obtained, this procedure is repeated. Eq. (4) is a mathematical model of the error function

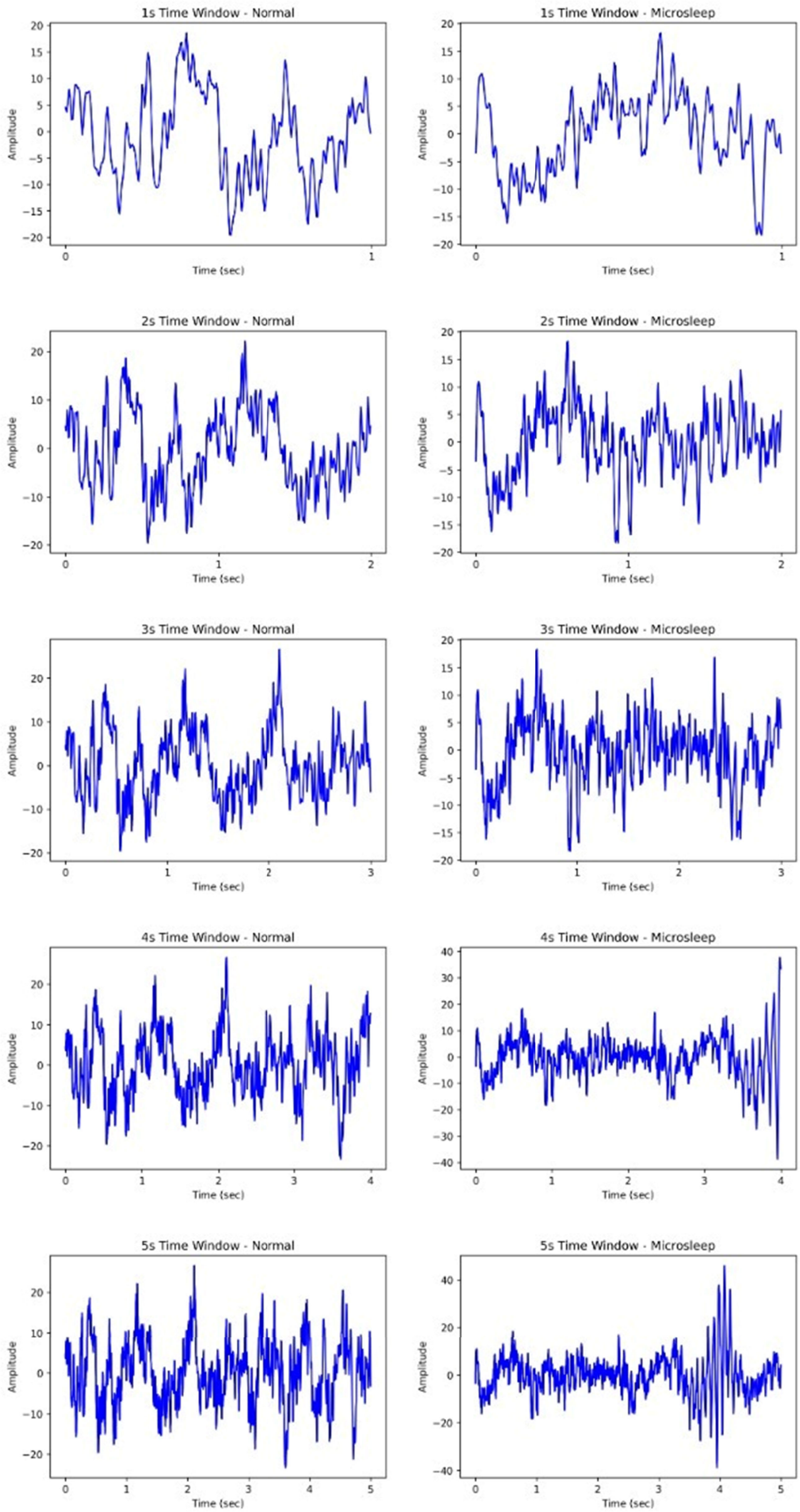

FIGURE 7. Example of five different time windows in the time domain for both normal and microsleep conditions. The signal patterns became more detailed for each sample, revealing additional fluctuations and variations in amplitude over longer durations, as the time window increases.

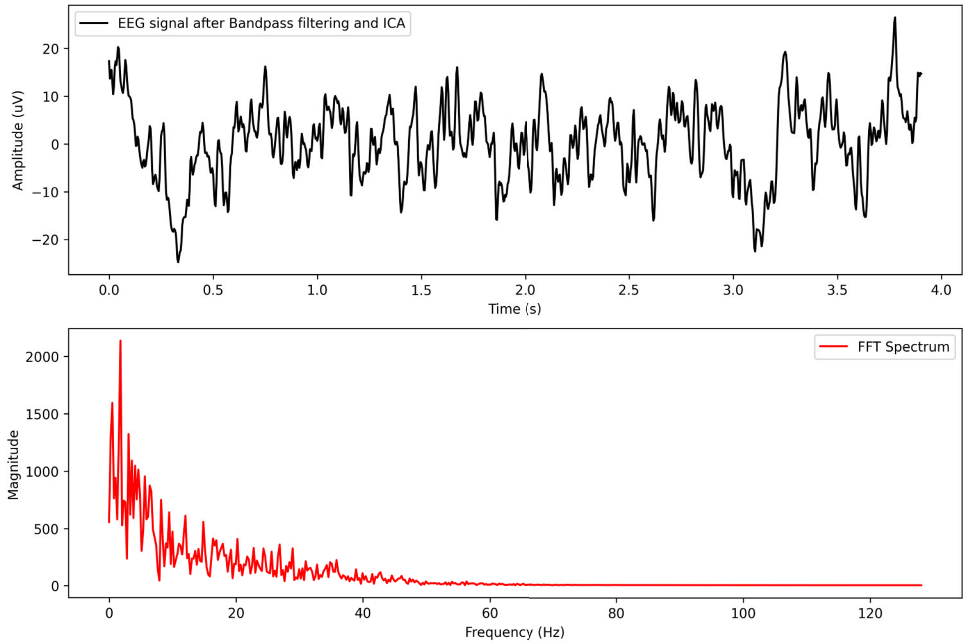

FIGURE 8. FFT Spectrum of EEG Signal after Bandpass Filtering and ICA. The FFT spectrum highlights the dominant frequency components, facilitating the identification of relevant oscillations.

derivatives utilized to modify the weights using gradient descent.

$$\Delta w(t) = \eta \nabla E(t) + \alpha \Delta w(t-1) \tag{4}$$

where E is the difference between the expected and actual outputs, η is the learning parameter, α is the momentum parameter (< 1), and Δw is the weight update. Based on the complexity of the problem, we move into the deep learning domain with each additional hidden layer [39].

Neural networks are frequently employed as successful supervised machine learning methods for classification issues in the context of reservoir characterization. This is mostly due to a special capacity of neural network to imitate human thought processes [40] to tackle classification difficulties by developing intricate dynamic estimate functions that outperform other methods. In theory, an ANN can learn the form of any function required for classification if sufficient processing power is provided.

The most frequent flaws in ANNs are their high processing power requirements, intricate construction, need for careful fine-tuning, curse of dimensionality, and tendency to become trapped at the local minima. The majority of these flaws were alleviated by hybrid ANN models [38]. Global minima occur when the weight of the loss function is the lowest at a point within the entire domain of the loss function, whereas local minima occur when the weight of the loss function is lowest at a point within a specific local domain. Several approaches have been proposed to overcome the weights that converge to local minima. Training neural networks with variable weights and growing iterations is one such method [41]. Another strategy is to start with a higher step size and use various local optimization methods, such as hill climbing, metaheuristic algorithms, and simulated annealing, to repeatedly reduce the step size [42]. Finding the global optimal solution in an ANN is a challenging task; however, new research indicates that the stochastic gradient descent approach is sufficiently effective [43].

D. HYPERPARAMETER TUNING

Hyperparameters are configurations of variables found outside a model that are established before the learning process begins. These are used to influence how a model's learning process is structured or operated. The fundamental method for enhancing the prediction accuracy of a model network is via training algorithm hyperparameter tuning: learning rate, epoch, iterations, mini-batch size, optimizer method, momentum, or neural network hyperparameters: increasing the number of hidden layers based on the output, dropout optimization, type of activation function, number of training epochs, and weight initialization. In machine learning or deep learning processes, hyperparameters are mostly selected by trial and error. Consequently, model performance is often measured by learning with different hyperparameter settings and testing against a validation dataset. The most common hyperparameter tuning strategies used in reservoir characterization are as follows.

- Heuristic-based: Typically based on trial and error.
- Random search: A simple yet efficient method for hyperparameter optimization, enabling broad exploration of parameter spaces to improve the model performance. As stated by [38], this provides a superior and

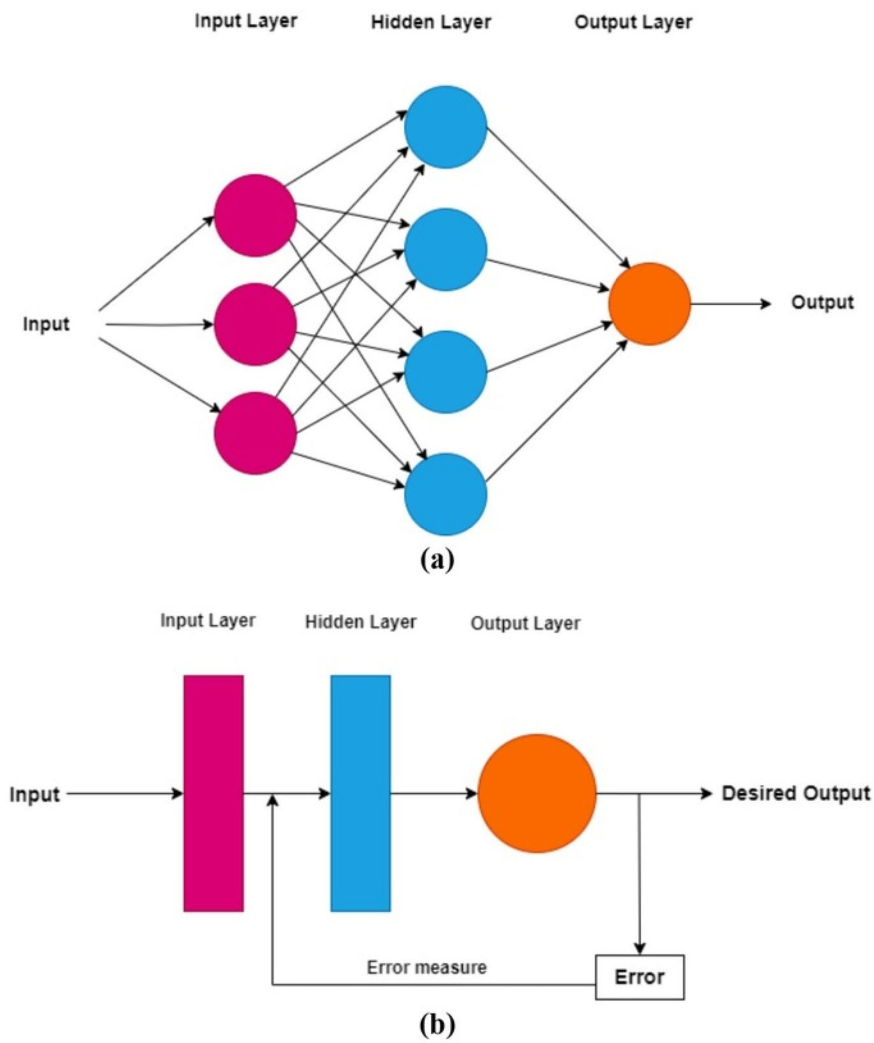

FIGURE 9. Neural Network architecture. (a) Typical Feed-Forward Neural Network. (b) Back-propagation Neural Network architecture showing the error being looped back through the network for weight tuning.

more successful approach for selecting hyperparameter values than manual and grid search methods.
- Grid search: This typically entails systematic retraining of the model with various combinations of hyperparameter values.
- Bayesian optimization: This approach monitors the form of functions produced via an iterative training procedure with varying hyperparameter values. The functions are then expanded and utilized to forecast the ideal hyperparameter values, providing more accuracy than random search [44].

E. PROPOSED HYPER-OPT-ANN MODEL

In this study, we introduce the Hyper-Opt-ANN model, a painstakingly built deep learning model for improving classification problems via rigorous hyperparameter optimization. The main design of the Hyper-Opt-ANN starts with an input layer, followed by densely connected layers, each optimized for performance through systematic adjustments to its hyperparameters. Fig. 10 provides a visual representation of the training process, detailing the steps involved to find the best configuration after a thorough hyperparameter optimization for microsleep detection.

The Hyper-Opt-ANN model is carefully designed to enhance classification tasks through meticulous hyperparameter optimization. Before identifying the best-performing model, the initial approach involved building the model using ‘‘RandomSearch’’ of Keras Tuner. This process systematically explores different combinations of model parameters, including the number of neurons in dense layers, dropout rates, and learning rates, to identify an optimal configuration for classification performance. The model architecture consist of an input layer processing eight features, followed by two dense layers with varying neuron counts (ranging from 32 to 128) and ReLU activation functions. Batch Normalization is applied to stabilize training, and Dropout layers

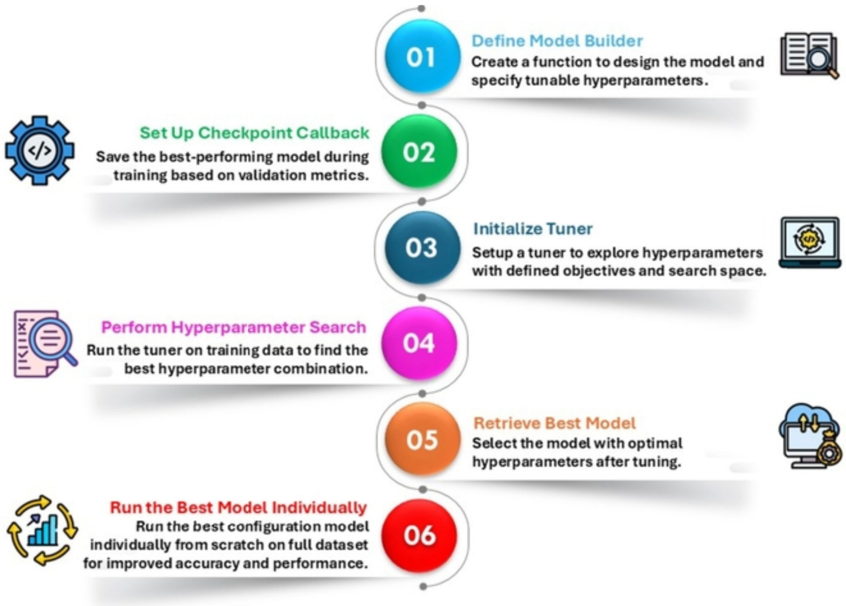

FIGURE 10. Training procedures of the proposed Hyper-Opt-ANN Model, detailing the steps involved to find the best configuration after a thorough hyperparameter optimization for microsleep detection.

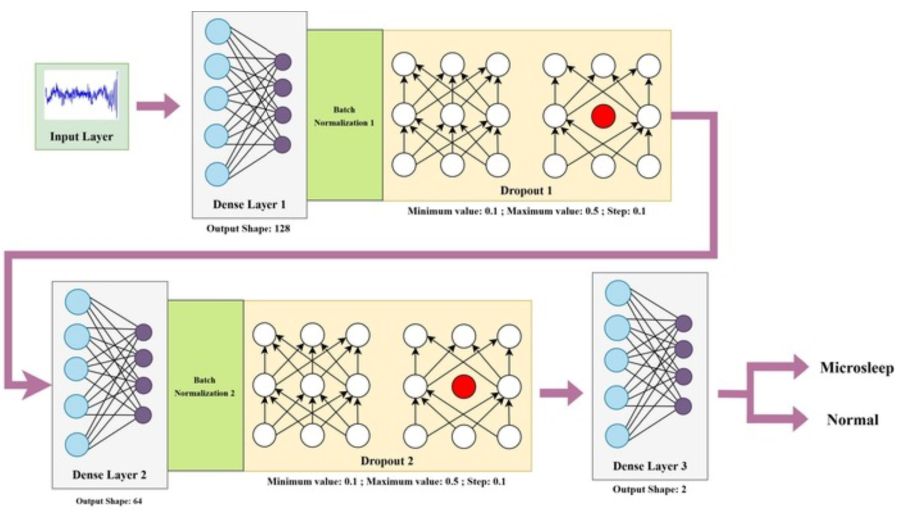

FIGURE 11. Proposed Hyper-Opt-ANN architecture. The proposed design enhances classification tasks through meticulous hyperparameter optimization.

(0.1 to 0.5) re incorporated to mitigate overfitting. The output layer employs a softmax activation for binary classification. The tuning process evaluates 20 different configurations, each repeated twice for reliability, and assesses performance based on validation accuracy. The Adam optimizer is used with a learning rate search space of 0.001, 0.0001, 0.00001, ensuring an adaptive and efficient weight update mechanism. The model undergoes 200 epochs of training, with early stopping monitoring validation accuracy to prevent unnecessary training iterations.

This hyperparameter tuning phase is critical in selecting an optimized model with the best-performing parameter set. Following this, the best configuration is extracted and used to develop an independent fixed-parameter model for further validation, ensuring that the optimization process yielded a robust and generalizable classification model. Fig. 11 depicts the architecture of the Hyper-opt-ANN model to detect microsleep.

After conducting hyperparameter tuning using Keras Tuner, the process identifies the best-performing configuration based on validation. This optimized model includes specific values for key hyperparameters, such as the number of units in each dense layer, dropout rates, and the learning rate. To further validate the model effectiveness, a separate experiment implements the best parameter model independently, without additional optimization. This approach ensures that the model performance is assessed solely based on the previously determined optimal parameters, eliminating any variability introduced by hyperparameter tuning.

V. RESULTS

To determine the ideal period for identifying microsleep occurrences using the suggested Hyper-Opt-ANN model, five distinct time frames were examined in this study. The choice of several time frames made it possible to evaluate which window size provided the greatest trade-off between prompt detection and reducing delays or false positives, which is an important factor for real-time applications such as driving safety systems. The EEG data from the 15 participants comprised the dataset, which was divided into training (80%) and testing (20%) classes. This study sought to determine the ideal window size for microsleep detection by evaluating the performance across various windows, ensuring dependability and usefulness in real-world situations.

A thorough evaluation of the proposed Hyper-Opt-ANN model for microsleep detection from EEG data was conducted over five different time windows. Accuracy, specificity, Matthews Correlation Coefficient (MCC), precision, recall, F1-score, and Cohen's kappa were among the important performance measures evaluated. The findings for all time windows are summarized in Fig. 12, demonstrating the resilience and flexibility of the model in differentiating between microsleep and normal states throughout a range of time periods.

The accuracy of the model for the 1s time window was 90.87%. The MCC, which reflects the balance between true and false predictions, was 81.93%, while specificity, which measures the ability to accurately identify non-microsleep conditions, was 94.52%. With a recall of 87.10% and precision of 93.90%, the model effectively minimizes false positives while successfully identifying actual microsleep occurrences. The model's reliability over brief time windows was further validated by an F1-score of 91.29% and Cohen's kappa of 82.64%.

Results from the 3s time window were even more remarkable. Specificity was 97.88%, with accuracy reaching 96.33%. The MCC increased to 92.59%, a critical measure of classification balance. The F1-score was 97.02%, with precision and recall values of 97.32% and 94.42%, respectively. This window demonstrated a high degree of agreement between predicted and actual classifications, as evidenced by a Cohen's kappa of 94.59%, indicating the model's effectiveness in distinguishing between microsleep and normal states.

The best overall performance was achieved with the 4s time window. Specificity was 98.75%, and accuracy reached 97.33%, demonstrating remarkable dependability for detecting non-microsleep conditions. The MCC was the highest across all time windows at 94.18%, indicating optimal balance in handling both positive and negative categories. The F1-score was exceptional at 97.85%, with a recall rate of 95.74% and precision of 98.54%. Cohen's kappa of 94.65% further underscores the accuracy and reliability of this time window, making it the most optimal for microsleep detection.

Although the 5s time window showed slightly lower performance than the 4s time window, it continued to perform well. Specificity was 99.45%, and accuracy was 96.94%. The MCC remained high at 93.99%, though it was slightly below the values for the 3s and 4s time windows. The recall was the highest of all time frames at 94.35%, while precision stood at 99.40%. This high recall rate demonstrates the model's strong capability in identifying microsleep occurrences. The performance in this time frame was further validated by an F1-score of 96.42% and Cohen's kappa of 92.78%, indicating continued effectiveness in classification..

However, Fig. 13 presents the overall accuracy and loss curves of the proposed Hyper-Opt-ANN model for both training and validation across various time windows. These curves provide a detailed visualization of the performance of the model over different durations, illustrating its ability to effectively learn and generalize during both the training and validation phases.

For the 1s time window, shown in Fig. 13(a) and Fig. 13(b), the training accuracy ranged from 89% to 92%, with a corresponding pattern observed in the validation accuracy. The model achieved peak performance at epoch 193. The consistent decline in training loss indicates efficient learning with minimal signs of overfitting. However, slight fluctuations in validation loss, ranging from 0.30 to 0.37, suggest some variability in validation performance.

In the 2s time window, depicted in Fig. 13(c) and Fig. 13(d), the model exhibited improved performance, with training and validation accuracies reaching 94% to 95%. The best performance was recorded at epoch 192. Although the validation loss exhibited greater variability, implying occasional fluctuations in validation performance, the steady decrease in training loss (falling below 0.16) indicates stable learning with no significant overfitting..

The 3s time window, presented in Fig. 13(e) and Fig. 13(f), demonstrated strong generalization capabilities. Both training and validation accuracies were closely aligned, with the loss curves converging at epoch 100. This convergence suggests a balanced trade-off between accuracy and loss, further affirming the robustness of the model. The training and validation accuracies were aligned at 94% and 96.3%, respectively, with the loss metrics stabilizing near 0.18 for both. This balance indicates that the model generalizes well without overfitting, making the 3s time window a strong candidate for applications requiring a balance between performance and computational efficiency.

The 4s time window, shown in Fig. 13(g) and Fig. 13(h), yielded the most favorable results. Training accuracy remained stable at 97%, while validation accuracy fluctuated but ultimately stabilized at 97.33%. The narrow gap between training and validation accuracy indicates exceptional generalization without overfitting. Both training and validation losses exhibited a steady decline, stabilizing at approximately 0.15, respectively. This time window emerged as optimal for

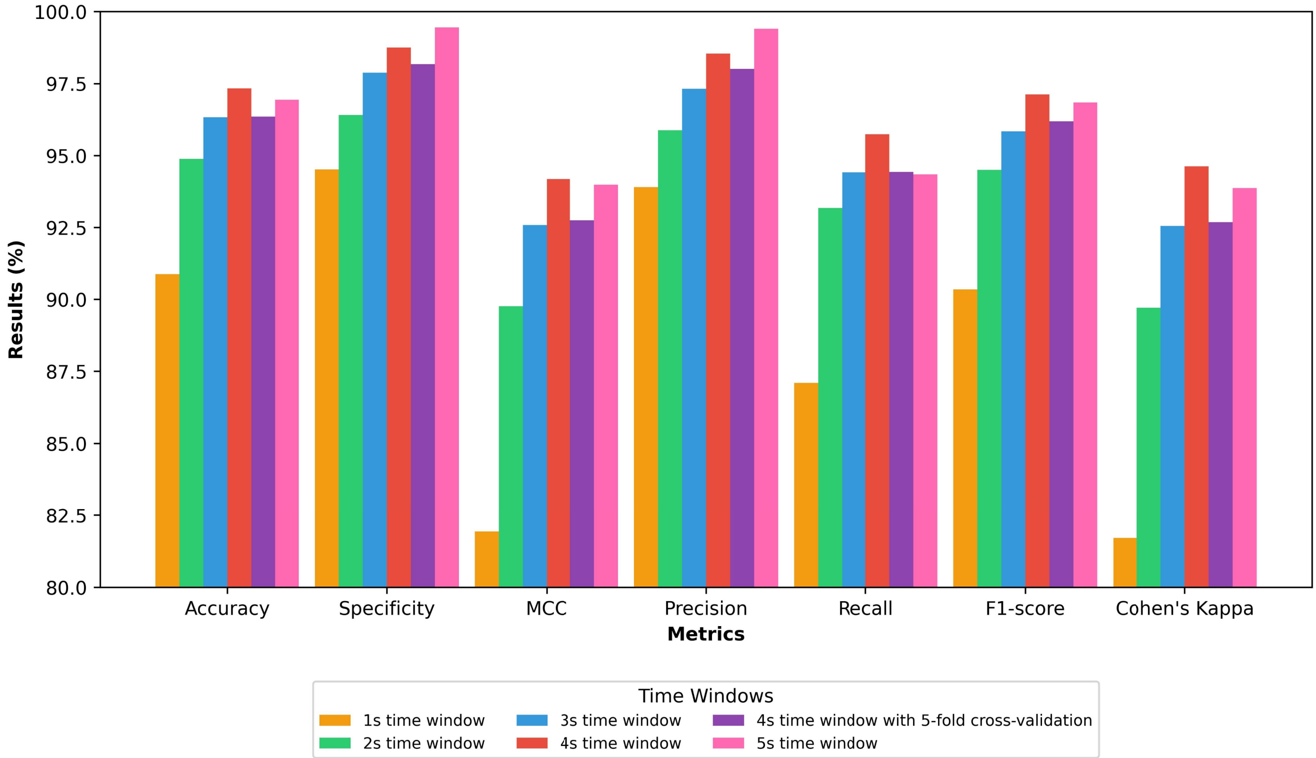

FIGURE 12. Comparison of performance evaluation metrics for the proposed model across different time windows. The achieved performance demonstrates the resilience and flexibility of the model in differentiating between microsleep and normal states throughout a range of time periods. The bar in purple shows the performance metrics after applying cross-validation. The results after applying 5-fold cross-validation are very similar to results for 4s time window without cross-validation.

detecting microsleep states, with peak performance observed at epoch 155.

Finally, Fig. 13(i) and Fig. 13(j) illustrate high performance for the 5s time window, where validation accuracy reached 96.94% and training accuracy fluctuated around 96% to 97%. The validation loss settled at 0.12, while the training loss stabilized at approximately 0.15. The model achieved its highest performance early in training at epoch 41, suggesting rapid acquisition of key patterns. The small difference between training and validation losses indicates sustained learning with minimal risk of overfitting.

In summary, the Hyper-Opt-ANN model demonstrated consistent and robust learning capabilities across all time windows, with the 4s time window emerging as the most effective for microsleep detection, achieving optimal performance.

Additionally, Fig. 14 illustrates the classification performance for identifying microsleep episodes from EEG signals across five time windows, using Receiver Operating Characteristic (ROC) curves. By plotting the True Positive Rate (TPR) against the False Positive Rate (FPR) for various classification thresholds, each ROC curve demonstrates the ability of the model to distinguish between microsleep and non-microsleep states.

In Fig. 14(a), the ROC curve for the 1s time window shows an Area Under the Curve (AUC) of 0.97, indicating strong discriminative power. The high AUC value suggests that the model effectively differentiates between microsleep and normal states, achieving accurate detection with minimal false positives. For the 2s time window, depicted in Fig. 14(b), the ROC curve achieves an AUC of 0.99, reflecting near-perfect discrimination. This performance highlights an optimal balance between specificity and sensitivity, minimizing false alarms while accurately classifying microsleep events. Similarly, in Fig. 14(c), the ROC curve for the 3s time window also demonstrates an AUC of 0.99, offering excellent classification performance. The steep rise of the curve toward the top-left corner further supports the strong sensitivity and low false-positive rate of the model, underscoring the durability of the model in detecting microsleep. The 4s time window, shown in Fig. 14(d), yields the highest performance, with a perfect AUC of 1.00, indicating flawless classification. The proximity of the ROC curve to the upper-left corner emphasizes the ideal balance between sensitivity and specificity, making the 4s time window highly effective for microsleep detection. Lastly, in Fig. 14(e), the ROC curve for the 5s time window maintains an AUC of 1.00, demonstrating flawless performance in distinguishing between microsleep and normal states. This result demonstrates that maintaining high classification accuracy across various time windows is achievable without compromising performance.

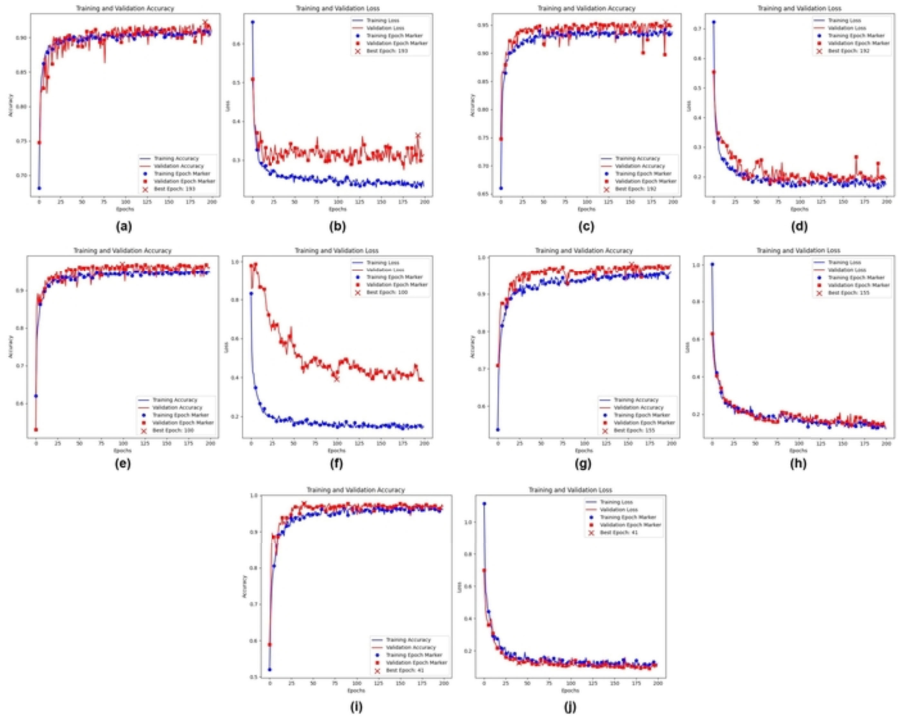

FIGURE 13. **Overall accuracy and loss curves of 200 epochs for both training and validation of the proposed model: (a) 1s accuracy, (b) 1s loss; (c) 2s accuracy, (d) 2s loss; (a) 2s accuracy, (f) 3s loss; (g) 4s accuracy, (h) 4s loss; (i) 5s accuracy, (j) 5s loss.**

The findings of this study indicate that the 4s time window is the best option for identifying microsleep, because it provides the optimum trade-off between generalization performance. This window is perfect for real-world applications such as driving safety systems because it enhances dependability while decreasing false positives. Because it showed the best general efficiency and dependability, the remaining performance of this investigation was concentrated on a 4s time window. Table 1 provides comprehensive details on the parameter optimization of the proposed Hyper-Opt-ANN model, identifying the optimal configuration for the best 4s time window.

The architectural choices of the Hyper-Opt-ANN model significantly affected its performance by balancing complexity and efficiency. The input layer processes 8-channel EEG signals, allowing the model to learn from multivariate data effectively. The first dense layer, with 96 neurones, captured complex patterns in the data, while batch normalization stabilized training and dropout prevented overfitting. The second dense layer, reduced to 32 neurones, focuses on dimensionality reduction while retaining the essential features. The output layer, with two neurones, handles the binary classification task, ensuring well-calibrated predictions. The total number of parameters of the model (13,128) and trainable parameters (4,290) reflect an efficient design that achieves a high testing accuracy (97.33%). These configurations enable robust feature learning, effective generalization, and computational efficiency, making the model suitable for real-time applications in microsleep detection.

TABLE 1. **Parameter specifications of proposed Hyper-Opt-ANN model for the best 4s time window.**

Layer (type)	Output shape	Parameter
InputLayer	(None, 8)	0
dense (Dense)	(None, 96)	864
batch_normalization (BatchNormalization)	(None, 96)	384
dropout (Dropout)	(None, 96)	0
dense_1 (Dense)	(None, 32)	3104
batch_normalization_1 (BatchNormalization)	(None, 32)	128
dropout_1 (Dropout)	(None, 32)	0
dense_2 (Dense)	(None, 2)	66
Total parameters: 13,128		
Trainable parameters: 4,290		
Non-trainable parameters: 256		
Optimizer parameters: 8,582		

Fig. 15 presents the confusion matrix, illustrating the performance of the proposed model within an optimal time window of 4s. The model was effective for classifying 202 microsleep occurrences (true positives) and 236 normal cases (true negatives). Only 9 cases of microsleep episodes were overlooked (false negatives), and only 3 cases of normal states were mistakenly identified as microsleep (false positives). This demonstrates a high degree of memory and precision, confirming the efficacy of the 4s time window in accuratley identifying microsleep occurrences.

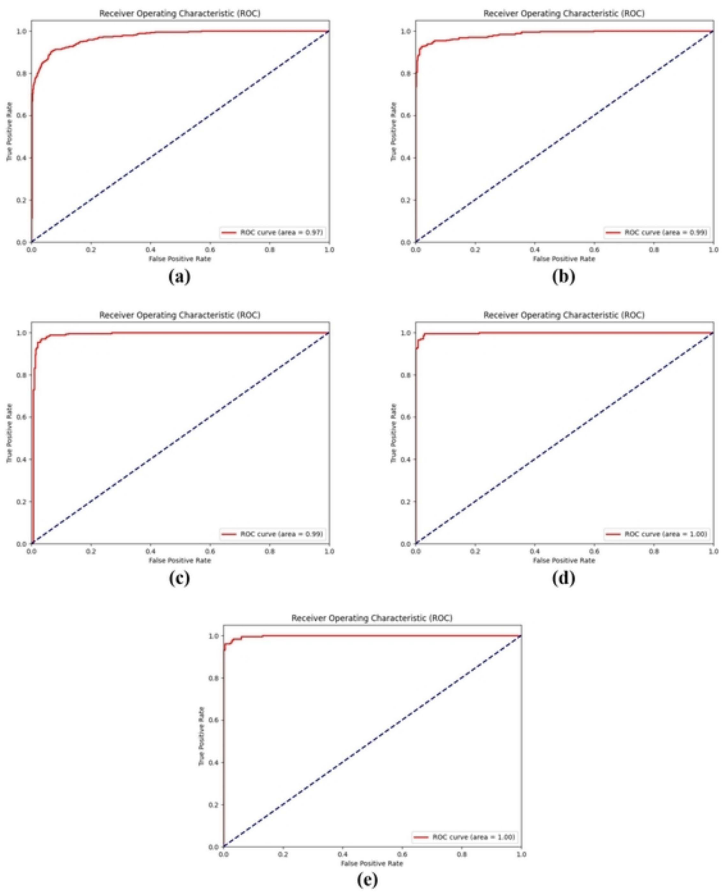

FIGURE 14. ROC curves of the proposed Hyper-Opt-ANN model across time windows (a) 1s, (b) 2s, (c) 3s, (d) 4s, and (e) 5s. The achieved performance demonstrates the ability of the model to distinguish between microsleep and non-microsleep states throughout a range of time periods.

TABLE 2. Individual performance of proposed model for the best 4s time window. The overall findings across accuracy, specificity, MCC, precision, recall, F1-score, and Cohen's Kappa were remarkable, with the exeption of Participants P-3 and P-6, which may be attributed to potential noise or outliers in their respective datasets.

Participants	Accuracy	Specificity	MCC	Precision	Recall	F1-score	Cohen's Kappa
P-1	0.98	0.98	0.97	0.99	0.99	0.99	0.97
P-2	0.97	1	0.94	1	0.95	0.97	0.95
P-3	0.94	0.99	0.88	0.98	0.90	0.94	0.88
P-4	0.97	0.98	0.94	0.98	0.96	0.97	0.95
P-5	0.96	0.97	0.87	0.97	0.90	0.93	0.87
P-6	0.93	0.97	0.87	0.97	0.90	0.93	0.87
P-7	1	1	1	1	1	1	1
P-8	1	1	1	1	1	1	1
P-9	1	1	1	1	1	1	1
P-10	1	1	1	1	1	1	1
P-11	0.99	0.98	0.98	0.98	1	0.99	0.99
P-12	0.98	0.98	0.96	0.98	0.97	0.98	0.96
P-13	1	1	1	1	1	1	1
P-14	0.98	1	0.97	1	0.97	0.98	0.97
P-15	0.99	0.98	0.98	0.98	1	0.99	0.99

The individual performance of the proposed Hyper-Opt-ANN model for the ideal 4s time window is shown in Table 2. With Participants P-7, P-8, P-9, and P-10 attaining perfect scores (100%) across all criteria, the results demonstrated excellent performance, and underscored the dependability of the method in these situations. The accuracy was consistently high for most people. Remarkably, 11 out of the 15 individuals achieved an accuracy of at least 98%. Even though their performance was still within acceptable bounds, Participant P-3 (94%) and Participant P-6 (93%), on the other hand, showed somewhat lower accuracy.

The results were almost immaculate in terms of specificity, which measures the capacity to accurately detect negative instances; Participants P-3 (0.99) and P-6 (0.97) displayed little variation. Among the participants, MCC, which considers both accurate and inaccurate predictions across classes, was also high. Participant P-6 had the lowest MCC score (0.87). Likewise, the majority of the individuals' accuracy levels were at or close to 1, suggesting very precise positive predictions. Participants P-6 (0.90) and P-3 (0.95) showed slight declines in recall performance, which measures the capacity to identify true positive cases, but the overall performance remained strong. F1-score, which showed somewhat lower values for P-3 (0.94) and P-6

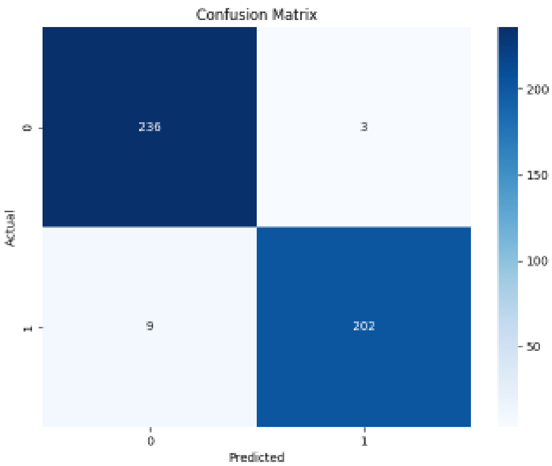

FIGURE 15. Confusion matrix of the proposed Hyper-Opt-ANN model for the best 4s time window. The model was effective for classifying 202 microsleep occurrences (true positives), 236 normal cases (true negatives), 9 false negatives, and only 3 false positives cases, confirming the efficacy of the 4s time window in accurately identifying microsleep.

(0.93), likewise showed this minor reduction. Cohen's Kappa, a measure of the degree of agreement between forecasts and actual results, differed among participants. Participants P-7 through P-10 obtained complete agreement (with values of 1); however, Participants P-3 (0.85) and P-6 (0.87) had relatively lower kappa levels.

Hence, the suggested technique exhibits exceptional performance, with little variation across all individuals. The overall findings across accuracy, specificity, MCC, precision, recall, F1-score, and Cohen's Kappa were still quite impressive, even though Participants P-3 and P-6 showed comparatively lower metrics. However, the observed low performance of participants P-3 and P-6 may be attributed to potential noise or outliers in their respective datasets. After excluding these two participants, the overall performance of the model showed a noticeable improvement, suggesting the robustness and accuracy of the model. This enhancement further underscores the significance of the model and its potential applicability in real-time scenarios, where precision and efficiency are paramount. This ensures constant and dependable performance within the 4s time window.

To further validate the proposed model, 5-fold cross-validation was applied to the optimal configuration for the 4s time window, ensuring a more comprehensive and reliable evaluation. This technique partitioned the dataset into K equally sized subsets ($K = 5$), with each subset serving as the test set while the remaining data was used for training. The results after applying 5-fold cross-validation are very similar to the previous results for 4s time window without cross-validation, with only slight differences. The performace metrics for the proposed model after applying cross-validation are illustrated in Fig. 12. The model still demonstrated strong performance, maintaining high values in key metrics such as accuracy 96.35% and specificity 98.17%. While there was a small decrease in precision 98.01% and recall 94.43%, the F1-score 96.19% and Cohen's Kappa 92.69% model after applying cross-validation showed minimal reduction. These results highlight the overall consistency and strong performance of the proposed model, confirming its reliability even after applying cross-validation.

VI. DISCUSSION

This research proposes a Hyper-Opt-ANN model based on microsleep detection, which achieves much better performance with a 4s time window than previous state-of-the-art studies. The average accuracy, specificity, MCC, precision, recall, F1-score, and Cohen's kappa of the proposed Hyper-Opt-ANN architecture were 98.00%, 98.33%, 95.99%, 98.10%, 97.63%, 98.87%, and 94.65%, respectively.

The findings of this study underscore the exceptional performance of the Hyper-Opt-ANN model in detecting microsleep episodes from EEG signals, particularly within the optimal 4-second time window. The model demonstrates a comprehensive and outstanding performance in accuracy, precision, recall, and F1-score metrics. These metrics are indispensable for assessing the robustness and applicability of the model. Precision reflects the model's ability to minimize false positives, recall indicates its sensitivity to actual microsleep states, and the F1-score captures the harmonic mean of these measures, providing a balanced performance assessment.

Moreover, the inherent "black-box" nature of deep learning models presents challenges to interpretability, which is critical for deployment in safety-critical systems. Future work should focus on integrating interpretable model techniques, such as saliency maps, layer-wise relevance propagation, or shapley value explanations, to elucidate the decision-making process. Interpretable insights into the activation of neural units or the relevance of features in detecting microsleep events could improve the reliability of the model and facilitate its integration into real-time decision support systems. This approach would not only improve transparency, but also ensure system accountability in high-stakes applications, such as driver alertness monitoring.

We also discovered that the duration of the time frame had a significant impact on the overall performance in this experiment. In contrast to the 1s, 2s, 3s, and 5s time windows, the study showed improvement in the 4s time window. To make an accurate choice and increase the efficacy in real-world applications, this study attempts to develop an effective network that can identify microsleep situations within an accurate time window. Table 3 shows a comparison between the suggested model and the existing research on microsleep-related studies.

The experimental results demonstrated that the proposed framework outperformed other relevant studies published in the literature. Previous studies have utilized a variety of EEG headsets with differing numbers of electrodes (ranging from 1 to 256) to detect microsleep states. To optimize the performance of the proposed model, it is important to

TABLE 3. Performance comparison of existing microsleep-related studies. The results demonstrate that the proposed framework outperform other relevant studies (using headsets with number of electrodes raging from 1 to 256) published in the literature.

Reference	Feature	Class	Algorithm	Accuracy
[45]	Raw EEG signal	2	CNN	94.00%
[46]	Empirical mode decomposition of multi-scale entropy	2	KNN	88.74%
[47]	Principal component analysis	2	SVM	86.00%
[26]	Tunable Q-factor wavelet transform	2	LSTM	94.31%
[48]	Fast Fourier transform	2	CNN	90.14%
[49]	Sequential forward floating of feature selection	2	RF	93.50%
[50]	CWT	2	CNN	88.85%
[51]	Short-time Welch transform	2	CNN	95.00%
[52]	Raw signal	2	CNN	78.35%
Our proposed model	FFT	2	Hyper-Opt-ANN	97.33%

determine the appropriate quantity and type of electrodes required. Future research should address these limitations by exploring the impact of different EEG headset configurations. This will help to validate the performance of the model and ensure its applicability to a broader range.

Even though the proposed method performs better than the most advanced microsleep detection techniques, particular challenges emerged during the experimental investigation. One key limitation is the small dataset used in this study, consisting of only 15 participants from a single institution. This limited sample size raises concerns about the generalizability of the findings. A more diverse and extensive dataset is essential to verify the viability of the proposed network across different populations and settings.

This proposed framework was also designed to minimize computational complexity while maintaining high accuracy, ensuring feasibility for real-time applications. The lightweight architecture enables rapid microsleep detection, reducing latency and allowing timely intervention to prevent accidents. Future work will focus on hardware optimization and integration with in-vehicle safety systems, such as Advanced Driver Assistance Systems (ADAS), to enhance real-time monitoring and intervention capabilities.

VII. CONCLUSION

This work presents an unique model, Hyper-Opt-ANN, designed for the accurate detection of microsleep from EEG signals. The proposed approach demonstrated outstanding performance, achieving 97.33% accuracy, 98.75% specificity, 94.18% MCC, 98.54% precision, 95.74% recall, 97.12% F1-score, and 94.63% Cohen's kappa within the optimal 4s time window. The key highlights of this study are as follows:

- Comprehensive evaluation of the model across different time windows (1s, 2s, 3s, 4s, 5s) to identify the optimal trade-off between prompt detection and high accuracy, which is crucial for real-world applications such as driver alertness monitoring.
- A detailed analysis of individual participant performance showed the consistency and robustness of the proposed approach, with most participants achieving near-perfect scores across various evaluation metrics.

Despite these promising results, this study has certain limitations. The dataset was relatively small and homogenous, which limited its generalizability. Future research should validate the model on larger, more diverse datasets and explore the impact of different EEG electrode configurations to balance the hardware complexity and accuracy. In addition, the computational demands of the Hyper-Opt-ANN model require further optimization for seamless real-time deployment in embedded systems. Improving model interpretability by using techniques such as saliency maps can enhance trust and usability in safety-critical applications. Addressing these limitations will pave the way for more robust, efficient, and practical microsleep detection solutions.

ETHICAL STATEMENT

Our experimental data got its ethical approval from IIUM Research Ethics Committee. Approval No: IREC 2023-239.

DATA AVAILABILITY

Data will be made available on request.

DECLARATION OF COMPETING INTEREST

The authors declare that they have no known competing financial interests or personal relationships that could have appeared to influence the work reported in this paper.

REFERENCES

[1] S. S. D. P. Ayyagari, R. D. Jones, and S. J. Weddell, "Detection of microsleep states from the EEG: A comparison of feature reduction methods," *Med. Biol. Eng. Comput.*, vol. 59, nos. 7–8, pp. 1643–1657, Jul. 2021, doi: 10.1007/s11517-021-02386-y.

[2] M. H. Zaky, R. Shoorangiz, G. R. Poudel, L. Yang, C. R. H. Innes, and R. D. Jones, "Increased cerebral activity during microsleeps reflects an unconscious drive to re-establish consciousness," *Int. J. Psychophysiology*, vol. 189, pp. 57–65, Jul. 2023, doi: 10.1016/j.ijpsycho.2023.05.349.

[3] U. Herrmann, C. Heß, A. G. Guggisberg, C. Roth, M. Gugger, and J. Mathis, "Sleepiness is not always perceived before falling asleep in healthy, sleep-deprived subjects," *Sleep Med.*, vol. 11, no. 8, pp. 747–751, Aug. 2010, doi: 10.1016/j.sleep.2010.03.015.

[4] O. M. Qureshi, A. Hafeez, and S. S. H. Kazmi, "Ahmedpur sharqia oil tanker tragedy: Lessons learnt from one of the biggest road accidents in history," *J. Loss Prevention Process Industries*, vol. 67, Sep. 2020, Art. no. 104243, doi: 10.1016/j.jlp.2020.104243.

[5] (2023). *Drivers Are Falling Asleep Behind the Wheel.* Accessed: Jun. 7, 2023. [Online]. Available: https://www.nsc.org/road/safety-topics/fatigued-driver

[6] R. D. Jones, G. R. Poudel, C. R. H. Innes, P. R. Davidson, M. T. R. Peiris, A. M. Malla, T. L. Signal, G. J. Carroll, R. Watts, and P. J. Bones, "Lapses of responsiveness: Characteristics, detection, and underlying mechanisms," in *Proc. Annu. Int. Conf. IEEE Eng. Med. Biol.*, Aug. 2010, pp. 1788–1791, doi: 10.1109/IEMBS.2010.5626385.

[7] A. Chougule, J. Shah, V. Chamola, and S. Kanhere, "Enabling safe ITS: EEG-based microsleep detection in VANETs," *IEEE Trans. Intell. Transp. Syst.*, vol. 24, no. 12, pp. 15773–15783, Dec. 2023, doi: 10.1109/TITS.2022.3230259.

[8] R. P. Balandong, R. F. Ahmad, M. N. Mohamad Saad, and A. S. Malik, "A review on EEG-based automatic sleepiness detection systems for driver," *IEEE Access*, vol. 6, pp. 22908–22919, 2018, doi: 10.1109/ACCESS.2018.2811723.

[9] S. Hu and G. Zheng, "Driver drowsiness detection with eyelid related parameters by support vector machine," *Expert Syst. Appl.*, vol. 36, no. 4, pp. 7651–7658, May 2009, doi: 10.1016/j.eswa.2008.09.030.

[10] Y. Tran, N. Wijesuriya, M. Tarvainen, P. Karjalainen, and A. Craig, "The relationship between spectral changes in heart rate variability and fatigue," *J. Psychophysiology*, vol. 23, no. 3, pp. 143–151, Jan. 2009, doi: 10.1027/0269-8803.23.3.143.

[11] M. Haghani, M. C. J. Bliemer, B. Farooq, I. Kim, Z. Li, C. Oh, Z. Shahhoseini, and H. MacDougall, "Applications of brain imaging methods in driving behaviour research," *Accident Anal. Prevention*, vol. 154, May 2021, Art. no. 106093, doi: 10.1016/j.aap.2021.106093.

[12] N. Naseer and K.-S. Hong, "FNIRS-based brain–computer interfaces: A review," *Frontiers Human Neurosci.*, vol. 9, pp. 1–11, Jan. 2015, doi: 10.3389/fnhum.2015.00003.

[13] M. J. Khan, M. J. Hong, and K.-S. Hong, "Decoding of four movement directions using hybrid NIRS-EEG brain–computer interface," *Frontiers Human Neurosci.*, vol. 8, no. 244, pp. 1–10, 2014, doi: 10.3389/fnhum.2014.00244.

[14] Z. Zhang, D. Luo, Y. Rasim, Y. Li, G. Meng, J. Xu, and C. Wang, "A vehicle active safety model: Vehicle speed control based on driver vigilance detection using wearable EEG and sparse representation," *Sensors*, vol. 16, no. 2, p. 242, Feb. 2016, doi: 10.3390/s16020242.

[15] J. Skorucak, A. Hertig-Godeschalk, D. R. Schreier, A. Malafeev, J. Mathis, and P. Achermann, "Automatic detection of microsleep episodes with feature-based machine learning," *Sleep*, vol. 43, no. 1, Jan. 2020, Art. no. zsz225, doi: 10.1093/sleep/zsz225.

[16] M. Golz, A. Schenka, F. Haselbeck, and M. P. Pauli, "Inter-individual variability of EEG features during microsleep events," *Current Directions Biomed. Eng.*, vol. 5, no. 1, pp. 13–16, Sep. 2019, doi: 10.1515/cdbme-2019-0004.

[17] G. C. Gutiérrez-Tobal, D. Álvarez, J. V. Marcos, F. del Campo, and R. Hornero, "Pattern recognition in airflow recordings to assist in the sleep apnoea–hypopnoea syndrome diagnosis," *Med. Biol. Eng. Comput.*, vol. 51, no. 12, pp. 1367–1380, Dec. 2013, doi: 10.1007/s11517-013-1109-7.

[18] G. Du, T. Li, C. Li, P. X. Liu, and D. Li, "Vision-based fatigue driving recognition method integrating heart rate and facial features," *IEEE Trans. Intell. Transp. Syst.*, vol. 22, no. 5, pp. 3089–3100, May 2021, doi: 10.1109/TITS.2020.2979527.

[19] K. Li, Y. Gong, and Z. Ren, "Vision-based fatigue driving recognition method integrating heart rate and facial features," *IEEE Trans. Intell. Transp. Syst.*, vol. 8, pp. 101244–1011259, 2020, doi: 10.1109/ACCESS.2020.2998363.

[20] M. Ramzan, H. U. Khan, S. M. Awan, A. Ismail, M. Ilyas, and A. Mahmood, "A survey on State-of-the-Art drowsiness detection techniques," *IEEE Access*, vol. 7, pp. 61904–61919, 2019, doi: 10.1109/ACCESS.2019.2914373.

[21] G. Lenis, P. Reichensperger, D. Sommer, C. Heinze, M. Golz, and O. Dössel, "Detection of microsleep events in a car driving simulation study using electrocardiographic features," *Current Directions Biomed. Eng.*, vol. 2, no. 1, pp. 283–287, Sep. 2016, doi: 10.1515/cdbme-2016-0063.

[22] M. K. Wali, M. Murugappan, and B. Ahmmad, "Wavelet packet transform based driver distraction level classification using EEG," *Math. Problems Eng.*, vol. 2013, pp. 1–10, Nov. 2013, doi: 10.1155/2013/297587.

[23] A. Garcés Correa, L. Orosco, and E. Laciar, "Automatic detection of drowsiness in EEG records based on multimodal analysis," *Med. Eng. Phys.*, vol. 36, no. 2, pp. 244–249, Feb. 2014, doi: 10.1016/j.medengphy.2013.07.011.

[24] S. N. Resalat and V. Saba, "A practical method for driver sleepiness detection by processing the EEG signals stimulated with external flickering light," *Signal, Image Video Process.*, vol. 9, no. 8, pp. 1751–1757, Nov. 2015, doi: 10.1007/s11760-015-0760-x.

[25] U. Budak, V. Bajaj, Y. Akbulut, O. Atila, and A. Sengur, "An effective hybrid model for EEG-based drowsiness detection," *IEEE Sensors J.*, vol. 19, no. 17, pp. 7624–7631, Sep. 2019, doi: 10.1109/JSEN.2019.2917850.

[26] C. Jacobé de Naurois, C. Bourdin, A. Stratulat, E. Diaz, and J.-L. Vercher, "Detection and prediction of driver drowsiness using artificial neural network models," *Accident Anal. Prevention*, vol. 126, pp. 95–104, May 2019, doi: 10.1016/j.aap.2017.11.038.

[27] F. Laurent, M. Valderrama, M. Besserve, M. Guillard, J.-P. Lachaux, J. Martinerie, and G. Florence, "Multimodal information improves the rapid detection of mental fatigue," *Biomed. Signal Process. Control*, vol. 8, no. 4, pp. 400–408, Jul. 2013, doi: 10.1016/j.bspc.2013.01.007.

[28] A. S. Houssaini, M. A. Sabri, H. Qjidaa, and A. Aarab, "Real-time Driver's hypovigilance detection using facial landmarks," in *Proc. Int. Conf. Wireless Technol., Embedded Intell. Syst. (WITS)*, Apr. 2019, pp. 1–4, doi: 10.1109/WITS.2019.8723768.

[29] X. Li, S. Lai, and X. Qian, "DBCFace: Towards pure convolutional neural network face detection," *IEEE Trans. Circuits Syst. Video Technol.*, vol. 32, no. 4, pp. 1792–1804, Apr. 2022, doi: 10.1109/TCSVT.2021.3082635.

[30] C. Gou, Y. Wu, K. Wang, K. Wang, F.-Y. Wang, and Q. Ji, "A joint cascaded framework for simultaneous eye detection and eye state estimation," *Pattern Recognit.*, vol. 67, pp. 23–31, Jul. 2017, doi: 10.1016/j.patcog.2017.01.023.

[31] J. Xu, J. Min, and J. Hu, "Real-time eye tracking for the assessment of driver fatigue," *Healthcare Technol. Lett.*, vol. 5, no. 2, pp. 54–58, Apr. 2018, doi: 10.1049/htl.2017.0020.

[32] J. J. Bird, L. J. Manso, E. P. Ribeiro, A. Ekárt, and D. R. Faria, "A study on mental state classification using EEG-based brain-machine interface," in *Proc. Int. Conf. Intell. Syst. (IS)*, Sep. 2018, pp. 795–800, doi: 10.1109/IS.2018.8710576.

[33] A. E. Manaenkov, N. O. Prokhorenko, O. N. Tkachenko, D. S. Sveshnikov, and V. B. Dorokhov, "Correlation of the Karolinska sleepiness with behavioral measures of a monotonous bimanual psychomotor rest," *Neurosci. Behav. Physiol.*, vol. 53, no. 9, pp. 1515–1520, Nov. 2023, doi: 10.1007/s11055-023-01547-w.

[34] M. Saeidi, W. Karwowski, F. V. Farahani, K. Fiok, R. Taiar, P. A. Hancock, and A. Al-Juaid, "Neural decoding of EEG signals with machine learning: A systematic review," *Brain Sci.*, vol. 11, no. 11, p. 1525, Nov. 2021, doi: 10.3390/brainsci11111525.

[35] X. Wang, V. Liesaputra, Z. Liu, Y. Wang, and Z. Huang, "An in-depth survey on deep learning-based motor imagery electroencephalogram (EEG) classification," *Artif. Intell. Med.*, vol. 147, Jan. 2024, Art. no. 102738, doi: 10.1016/j.artmed.2023.102738.

[36] E. C. Djamal, W. I. Furi, and F. Nugraha, "Detection of EEG signal post-stroke using FFT and convolutional neural network," in *Proc. 6th Int. Conf. Electr. Eng., Comput. Sci. Informat. (EECSI)*, Sep. 2019, pp. 18–23, doi: 10.23919/EECSI48112.2019.8977126.

[37] S. D. Mohaghegh, R. Arefi, I. Bilgesu, S. Ameri, and D. M. Rose, "Design and development of an artificial neural network for estimation of formation permeability," in *Proc. Petroleum Comput. Conf.*, vol. 7, Dec. 1995, pp. 151–154, doi: 10.2118/28237-pa.

[38] D. A. Otchere, T. O. Arbi Ganat, R. Gholami, and S. Ridha, "Application of supervised machine learning paradigms in the prediction of petroleum reservoir properties: Comparative analysis of ANN and SVM models," *J. Petroleum Sci. Eng.*, vol. 200, May 2021, Art. no. 108182, doi: 10.1016/j.petrol.2020.108182.

[39] P. Saikia, R. D. Baruah, S. K. Singh, and P. K. Chaudhuri, "Artificial neural networks in the domain of reservoir characterization: A review from shallow to deep models," *Comput. Geosci.*, vol. 135, Feb. 2020, Art. no. 104357, doi: 10.1016/j.cageo.2019.104357.

[40] S. Bhattacharya, P. K. Ghahfarokhi, T. R. Carr, and S. Pantaleone, "Application of predictive data analytics to model daily hydrocarbon production using petrophysical, geomechanical, fiber-optic, completions, and surface data: A case study from the Marcellus shale, North America," *J. Petroleum Sci. Eng.*, vol. 176, pp. 702–715, May 2019, doi: 10.1016/j.petrol.2019.01.013.

[41] W. Cao, X. Wang, Z. Ming, and J. Gao, "A review on neural networks with random weights," *Neurocomputing*, vol. 275, pp. 278–287, Jan. 2018, doi: 10.1016/j.neucom.2017.08.040.

[42] C. C. Kerr, S. Dura-Bernal, T. G. Smolinski, G. L. Chadderdon, and D. P. Wilson, "Optimization by adaptive stochastic descent," *PLoS ONE*, vol. 13, no. 3, Mar. 2018, Art. no. e0192944, doi: 10.1371/journal.pone.0192944.

[43] S. Liu, A. Borovykh, L. A. Grzelak, and C. W. Oosterlee, "A neural network-based framework for financial model calibration," *J. Math. Ind.*, vol. 9, no. 1, pp. 1–28, Dec. 2019, doi: 10.1186/s13362-019-0066-7.

[44] B. Shahriari, K. Swersky, Z. Wang, R. P. Adams, and N. de Freitas, "Taking the human out of the loop: A review of Bayesian optimization," *Proc. IEEE*, vol. 104, no. 1, pp. 148–175, Jan. 2016, doi: 10.1109/JPROC.2015.2494218.

[45] V. P. Balam, V. U. Sameer, and S. Chinara, "Automated classification system for drowsiness detection using convolutional neural network and electroencephalogram," *IET Intell. Transp. Syst.*, vol. 15, no. 4, pp. 514–524, Apr. 2021, doi: 10.1049/itr2.12041.

[46] S. Zou, T. Qiu, P. Huang, X. Bai, and C. Liu, ''Constructing multi-scale entropy based on the empirical mode Decomposition(EMD) and its application in recognizing driving fatigue,'' *J. Neurosci. Methods*, vol. 341, Jul. 2020, Art. no. 108691, doi: 10.1016/j.jneumeth.2020.108691.

[47] A. Chaudhuri and A. Routray, ''Driver fatigue detection through chaotic entropy analysis of cortical sources obtained from scalp EEG signals,'' *IEEE Trans. Intell. Transp. Syst.*, vol. 21, no. 1, pp. 185–198, Jan. 2020, doi: 10.1109/TITS.2018.2890332.

[48] S. Chaabene, B. Bouaziz, A. Boudaya, A. Hökelmann, A. Ammar, and L. Chaari, ''Convolutional neural network for drowsiness detection using EEG signals,'' *Sensors*, vol. 21, no. 5, p. 1734, Mar. 2021, doi: 10.3390/s21051734.

[49] H. Martensson, O. Keelan, and C. Ahlström, ''Driver sleepiness classification based on physiological data and driving performance from real road driving,'' *IEEE Trans. Intell. Transp. Syst.*, vol. 20, no. 2, pp. 421–430, Feb. 2019, doi: 10.1109/TITS.2018.2814207.

[50] Y. Wang, Y. Huang, B. Gu, S. Cao, and D. Fang, ''Identifying mental fatigue of construction workers using EEG and deep learning,'' *Autom. Construction*, vol. 151, Jul. 2023, Art. no. 104887, doi: 10.1016/j.autcon.2023.104887.

[51] J. Shah, A. Chougule, V. Chamola, and A. Hussain, ''Novel welch-transform based enhanced spectro-temporal analysis for cognitive microsleep detection using a single electrode EEG,'' *Neurocomputing*, vol. 549, Sep. 2023, Art. no. 126387, doi: 10.1016/j.neucom.2023.126387.

[52] J. Cui, Z. Lan, O. Sourina, and W. Müller-Wittig, ''EEG-based cross-subject driver drowsiness recognition with an interpretable convolutional neural network,'' *IEEE Trans. Neural Netw. Learn. Syst.*, vol. 34, no. 10, pp. 7921–7933, Oct. 2023, doi: 10.1109/TNNLS.2022.3147208.

MD MAHMUDUL HASAN received the B.Sc. degree in electrical and electronic engineering from Jashore University of Science and Technology, Bangladesh, in 2021. He is currently pursuing the M.Sc. (research-based) degree with the Faculty of Electrical and Electronics Engineering Technology, Universiti Malaysia Pahang Al-Sultan Abdullah, Malaysia.

Upon completing his B.Sc. degree, he joined the Energy Research Laboratory, Jashore University of Science and Technology, as a Research Assistant, where he worked, until 2022. From 2022 to 2023, he was a Service Engineer with M. Rahman & Company Ltd., Bangladesh. He is currently a Graduate Research Assistant and a Teaching Assistant with Universiti Malaysia Pahang Al-Sultan Abdullah. His research interests include biomedical signal processing, image processing, machine learning, and deep learning. He was a recipient of the Holistic Incentive Scheme Scholarship from Universiti Malaysia Pahang Al-Sultan Abdullah.

MD NAHIDUL ISLAM received the B.Sc. degree in electrical and electronic engineering from Jashore University of Science and Technology, Bangladesh, in 2019. He is currently pursuing the M.Sc. degree with the Faculty of Electrical and Electronics Engineering Technology, University Malaysia Pahang Al-Sultan Abdullah, Malaysia.

He is currently a Graduate Research Assistant with the Faculty of Electrical and Electronics Engineering Technology, Universiti Malaysia Pahang Al-Sultan Abdullah. His research interests include brain–computer interface, artificial intelligence, biomedical signal processing, image processing, machine learning, and deep learning. He received the Postgraduate Research Grant Scheme Scholarship from Universiti Malaysia Pahang Al-Sultan Abdullah.

NORIZAM SULAIMAN received the B.Sc. degree in computer engineering from Valparaiso University, USA, in 1995, the M.Sc. degree in electronic systems design from University Sains Malaysia, Malaysia, in 2005, and the Ph.D. degree in electrical engineering from University Technology MARA, Malaysia, in 2015.

He has eight years working experience as an Engineer in multinational company, from 1995 to 2003. Since 2005, he has been a Senior Lecturer and attached to the Faculty of Electrical and Electronics Engineering Technology, Universiti Malaysia Pahang Al-Sultan Abdullah, Malaysia. His research interests include biomedical signal processing, image processing, and machine learning.

Dr. Sulaiman was awarded the Charted Engineer (CEng) by the Engineering Council, U.K., in April 2018, and a Professional Engineer by Board of Engineers Malaysia, in July 2019. He has been a Corporate Member of the Institution of Engineers, Malaysia, since April 2016, and become a Professional Technologist of Malaysia, Board of Technologists, in February 2018.

MIRZA MAHFUJ HOSSAIN received the B.Sc. degree in computer science and engineering from Jashore University of Science and Technology, Bangladesh, in 2025.

He is currently a Research Assistant with the JUST VMI Laboratory. His research interests include deep learning, signal processing, and medical image segmentation.

JORGE M. MENDES received the B.Sc. degree in statistics and information management from the NOVA Information Management School (NOVAIMS), NOVA University Lisbon, in 1997, the M.Sc. degree in probability and statistics, in 2000, and the Ph.D. degree in statistics and operations research from the University of Lisbon, Lisbon, in 2006.

He was a Research Assistant and an Assistant Professor with NOVAIMS, NOVA University of Lisbon, from 1997 to 2006 and from 2006 to 2018, respectively. From 2019 to 2023, he was an Associate Professor with NOVAIMS. Since 2024, he has been an Associate Professor with the NOVA Medical School, Nova University Lisbon. He is the author of more than 60 articles and frequently supervises the M.Sc. and Ph.D. students. He is also leading a research stream in artificial intelligence in healthcare with the Comprehensive Health Research Centre (CHRC). His research interests include spatial analysis, sampling theory, spatial epidemiology, and machine learning. He is a reviewer of several journals and is often invited as an external examiner in academic examinations.

Dr. Mendes was a recipient of several awards in his career, of which the Grand Bial Award of Medicine, in 2016.